Occult Scaphoid Fractures: Comparison of Multidetector CT and MR Imaging—Initial Experience[1]

Mazda Memarsadeghi, MD
Martin J. Breitenseher, MD
Cornelia Schaefer-Prokop, MD
Michael Weber, MS
Silke Aldrian, MD
Christian Gäbler, MD
Mathias Prokop, MD

Purpose: To compare the diagnostic performance of multidetector computed tomography (CT) and magnetic resonance (MR) imaging in patients clinically suspected of having a scaphoid fracture and who had normal initial radiographs, with radiographs obtained 6 weeks after trauma as the reference standard.

Materials and Methods: The ethics committee approved the study, and all patients gave written informed consent. Twenty-nine patients (17 male, 12 female; age range, 17–62 years; mean age, 34 years ± 13) underwent multidetector CT and MR imaging within 6 days after trauma. CT data were obtained with 0.5-mm collimation. For image review, 0.7-mm-thick multiplanar reformations were performed in transverse, coronal, and sagittal planes relative to the wrist. The 1.0-T MR examination consisted of coronal and transverse short inversion time inversion-recovery, coronal and transverse T1-weighted spin-echo, and coronal volume-rendered T2-weighted gradient-echo sequences. Two radiologists analyzed the CT and MR images. A binomial test was used to evaluate the significance of the differences between MR imaging and CT in detection of scaphoid fractures and cortical involvement ($P < .05$).

Results: The 6-week follow-up radiographs depicted a scaphoid fracture in 11 (38%) patients. Eight patients had a cortical fracture, while three patients had only a bandlike lucency within the trabecular portion of the scaphoid. MR imaging depicted all 11 fractures but only two cortical fractures. Multidetector CT depicted all eight cortical fractures but failed to depict trabecular fractures. No false-positive fractures were seen on MR or CT images. Differences between MR imaging and CT were not significant for the detection of scaphoid fractures ($P = .25$) but were significant for cortical involvement ($P = .03$).

Conclusion: Multidetector CT is highly accurate in depicting occult cortical scaphoid factures but appears inferior to MR imaging in depicting solely trabecular injury. MR imaging is inferior to multidetector CT in depicting cortical involvement.

[1] From the Departments of Radiology (M.M., M.J.B., C.S., M.W., M.P.) and Traumatology (S.A., C.G.), Medical University of Vienna, General Hospital of Vienna, Waehringer Guertel 18-20, A-1090 Vienna, Austria. Received March 11, 2005; revision requested May 4; revision received May 31; accepted June 21; final version accepted August 25. **Address correspondence to** M.M. (e-mail: *mazda.memarsadeghi@meduniwien.ac.at*).

© RSNA, 2006

The diagnosis of a scaphoid fracture can usually be established on the basis of clinical presentation and conventional radiographs. In cases of negative or equivocal findings, additional projections (ie, scaphoid views) and/or magnification views have been reported to increase sensitivity (1–3). However, immediately after injury, up to 65% of scaphoid fractures remain radiographically occult (1). For patients with a high clinical probability of a scaphoid fracture but unremarkable radiographs, it is therefore a common practice to place the wrist in a scaphoid cast until the scaphoid fracture is ruled out on follow-up radiographs obtained 2, 4, and 6 weeks after the trauma (1–8). If no fracture is visible on radiographs 6 weeks after trauma, it is considered safe to discontinue immobilization. This strategy, however, includes weeks-long unnecessary immobilization in some patients, which results in both a reduction in the quality of life and an increase in health care costs (9–11).

Other diagnostic tools such as scintigraphy, computed tomography (CT), intrasound vibration (ie, transcutaneous application of audible vibrations by using a 200–8500-Hz probe placed on the snuff box, which reportedly causes pain in patients with a scaphoid fracture), and ultrasonography have been proposed as second-line diagnostic tools (12–19) for patients clinically suspected of having a scaphoid fracture but with negative or equivocal findings on conventional radiographs obtained immediately after trauma. Because of its excellent sensitivity (95%–100%) and specificity (100%), magnetic resonance (MR) imaging has been advocated as the imaging modality of choice in these patients (9,13,20–24). MR imaging is exquisitely sensitive in depicting bone marrow abnormalities and therefore easily displays even nondisplaced fractures (23–25). MR imaging, however, may be limited in some patients because of the presence of indwelling electric devices or ferromagnetic objects, such as prostheses, or as a result of motion artifacts.

Multidetector CT may be an alternative imaging modality in patients with occult scaphoid fractures. It allows coverage of the whole wrist with isotropic spatial resolution (26). Single-detector CT has already been demonstrated to be more sensitive than radiography performed 6 weeks after trauma (27,28). To our knowledge, however, there is, to date, no clinical study in which multidetector CT was compared with MR imaging in patients with potential occult scaphoid fractures in the immediate posttraumatic phase. Thus, the purpose of our study was to compare the diagnostic performance of multidetector CT and MR imaging in patients clinically suspected of having a scaphoid fracture and who had normal initial radiographs, with radiographs obtained 6 weeks after trauma as the reference standard.

Advances in Knowledge

- Multidetector CT is superior to MR imaging for the detection of cortical involvement of occult scaphoid fractures.
- MR imaging is better than multidetector CT for detecting all scaphoid fractures.

Materials and Methods

Patients

Between June 2000 and July 2002, 29 patients (17 male, 12 female; age range, 17–62 years; mean age, 34 years ± 13) with negative initial posttrauma conventional radiographs were examined with multidetector CT and MR imaging. Both examinations were performed on the same day and 1–6 days after the initial trauma (mean, 4.1 days). All patients had trauma to the wrist, with subsequent severe pain over the scaphoid. The initial radiographs were obtained in four planes ("scaphoid views") 1–3 days (mean, 1.5 days) after the trauma and were first evaluated by two experienced trauma surgeons (S.A. and C.G., with 7 and 20 years, respectively, of experience in trauma surgery) and then by the same two radiologists (M.M., M.J.B.) who evaluated the MR and CT images. Only if the initial radiographs were negative for a fracture were the patients prospectively included in this study. The ethics committee of our institution approved the study, and all patients gave written informed consent.

According to our standard clinical procedure, follow-up scaphoid radiographs were obtained 2, 4, and 6 weeks after trauma. Therapeutic decisions (various degrees of immobilization) were based on clinical findings and on follow-up radiographs, also according to our standard clinical practice. Trauma surgeons were blinded to the interpretation of multidetector CT and MR images.

Imaging Technique

Radiographic examinations.—The initial radiographs and the follow-up radiographs consisted of the following four views: posteroanterior with the wrist in neutral position, lateral, semipronated oblique scaphoid, and radial oblique scaphoid. All radiographs were obtained by using a digital technique and a computed radiography system (Horizontal Diagnostic Super 80 CP; Philips Medical Systems, Eindhoven, the Netherlands), with a 0.1-mm pixel size and an exposure corresponding to a 100-speed radiography system at 45 kVp. Images were evaluated on film hard copies.

MR examination.—All MR images were obtained by using a 1.0-T unit (Gyroscan T10-NT; Philips Medical Systems) with appropriate receive-only surface coils. The standard imaging pro-

Published online
10.1148/radiol.2401050412

Radiology 2006; 240:169–176

Abbreviations:
CI = confidence interval
STIR = short inversion time inversion recovery

Author contributions:
Guarantors of integrity of entire study, all authors; study concepts/study design or data acquisition or data analysis/interpretation, all authors; manuscript drafting or manuscript revision for important intellectual content, all authors; approval of final version of submitted manuscript, all authors; literature research, M.J.B., C.S., C.G.; clinical studies, M.J.B., S.A., C.G., M.P.; statistical analysis, M.W.; and manuscript editing, M.J.B., C.S., C.G., M.P.

Authors stated no financial relationship to disclose.

tocol comprised a coronal and transverse short inversion time inversion-recovery (STIR) sequence (repetition time msec/echo time msec/inversion time msec, 1200/13/130; 2.4-mm section thickness), coronal and transverse T1-weighted spin-echo sequence (repetition time msec/echo time msec, 500/20; 2.4-mm section thickness), and coronal three-dimensional T2-weighted gradient-echo high-spatial-resolution sequence (60/17, 20° flip angle, 1.5-mm section thickness). A field of view of 140 mm with a 256 × 256 matrix was used for all sequences. All wrists were examined with the patient prone and the affected arm above the body.

Multidetector CT examination.—Multidetector CT was performed with a four–detector row scanner (Somatom Volume Zoom; Siemens, Forchheim, Germany), a detector configuration of two sections at 0.5 mm section thickness, 0.75-second rotation time, and a table feed of 1.5 mm per gantry rotation (pitch, 1.5). The tube voltage was 120 kVp, and the effective tube-current–time product was 120 mAs. The scan covered the wrist and parts of the hand, starting at the distal end of the radius proximal to the radiocarpal joint and covering at least the carpometacarpal joints. All affected wrists were positioned in a way similar to that used during MR imaging, with the patient prone and the affected arm above the body. No intravenous contrast material was injected.

Images were reconstructed by using a high-resolution convolution kernel (B90) and a 512 × 512 matrix. The field of view (range, 8–12 cm; mean, 9.5 cm) was adapted to the individual patient's anatomy. All scans were reconstructed with an effective section width of 0.5 mm and a reconstruction increment of 0.3 mm. For diagnostic evaluation, multiplanar reformations of 0.7-mm thickness were calculated in coronal, sagittal, and transverse planes relative to the wrist by using the standard software provided with the scanner (Volume Wizard; Siemens). For display, a bone window setting with a center of 600 HU and width of 1600 HU was chosen.

Image Evaluation

The sets of multidetector CT and MR images were retrospectively and independently reviewed by a 5th-year resident (M.M.) and a board-certified radiologist (M.J.B.), the latter with 20 years of experience in reading musculoskeletal CT and MR images. Any CT or MR image that was rated differently by the two observers was reevaluated by both readers together to reach a consensus opinion. In three (10.3%) of 29 cases, a consensus opinion was needed.

The readers separately determined the presence of a scaphoid fracture in the proximal, middle, or distal part of the scaphoid bone. Further, the readers distinguished between signs of a cortical and signs of a trabecular fracture. To approximate the clinical situation, the readers were informed about the site of clinical symptoms. In addition, readers were asked to note any other signs of bone injury in the region of the wrist.

Two reading sessions were performed. In each reading session, either multidetector CT or MR images were presented for each patient. The reading order with respect to patients and protocols was randomized and varied between the two readers. The interval between the reading sessions was 3–5 weeks. Readers evaluated the images at a diagnostic workstation (IMPAX DS

Table 1

Pattern of Scaphoid Fracture Seen in 11 of 29 Patients

Patient No./Age (y)	Follow-up Radiography	MR Imaging	Multidetector CT
1/24	Trabecular	Trabecular	No fracture
4/22	Cortical	Trabecular	Cortical
5/25	Cortical	Cortical	Cortical
6/23	Trabecular	Trabecular	No fracture
7/29	Cortical	Trabecular	Cortical
12/22	Cortical	Trabecular	Cortical
13/54	Cortical	Trabecular	Cortical
19/22	Trabecular	Trabecular	No fracture
25/38	Cortical	Cortical	Cortical
26/36	Cortical	Trabecular	Cortical
28/29	Cortical	Trabecular	Cortical

Table 2

Pattern of Fractures of Other Wrist Bones Seen in 13 of 29 Patients

Patient No./Age (y)	Fractured Bone	Follow-up Radiography	MR Imaging	Multidetector CT
6/23	Capitate	Trabecular	Trabecular	No fracture
9/40	Distal radius	Trabecular	Trabecular	No fracture
11/58	Hamate	Trabecular	Trabecular	No fracture
13/54	Distal radius	Trabecular	Trabecular	No fracture
14/26	Distal radius	Trabecular	Trabecular	No fracture
15/21	Distal radius	Trabecular	Trabecular	No fracture
16/44	Distal radius	Trabecular	Trabecular	No fracture
17/28	Lunate	Cortical	Cortical	Cortical
20/33	Distal radius	Cortical	Cortical	Cortical
21/34	Lunate	Cortical	Cortical	Cortical
22/30	Pisiform	Cortical	No fracture	Cortical
22/30	Triquetral	Cortical	No fracture	Cortical
26/36	Triquetral	Trabecular	Trabecular	No fracture

3000; Agfa Health Care, Mortsel, Belgium) by using an interactive mouse-driven cine mode. The ambient light was subdued, and there was no time constraint for reading. The observers were blinded to the results of follow-up radiographs.

Criteria for a bone fracture on MR images included the presence of a cortical fracture line, a trabecular fracture line, or a combination of both (14). Such a fracture line had to be evidenced by linear disruption of the normal trabecular pattern and had to be hyperintense on STIR and T2-weighted images and hypointense or hyperintense on T1-weighted images. Evidence of a zone of diffusely increased signal intensity on STIR images was interpreted as bone marrow edema but not as a manifest fracture (29).

Criteria for a bone fracture on multidetector CT images were the presence of a sharp lucent line within the trabecular bone pattern, a break in the continuity of the cortex, a sharp step in the cortex, or a dislocation of bone fragments.

Table 3

Detection of Occult Scaphoid Fractures in 29 Patients

Variable	Sensitivity (%)	Specificity (%)	Accuracy (%)
MR imaging			
All fractures	100 (11/11)	100 (18/18)	100 (29/29)
Cortical fractures	38 (3/8)	100 (3/3)	55 (6/11)
Multidetector CT			
All fractures	73 (8/11)	100 (18/18)	89 (26/29)
Cortical fractures	100 (8/8)	100 (3/3)	100 (11/11)

Note.—Numbers in parentheses were used to calculate the percentage. Specificity and accuracy were calculated by using both cortical and trabecular fractures.

Figure 1

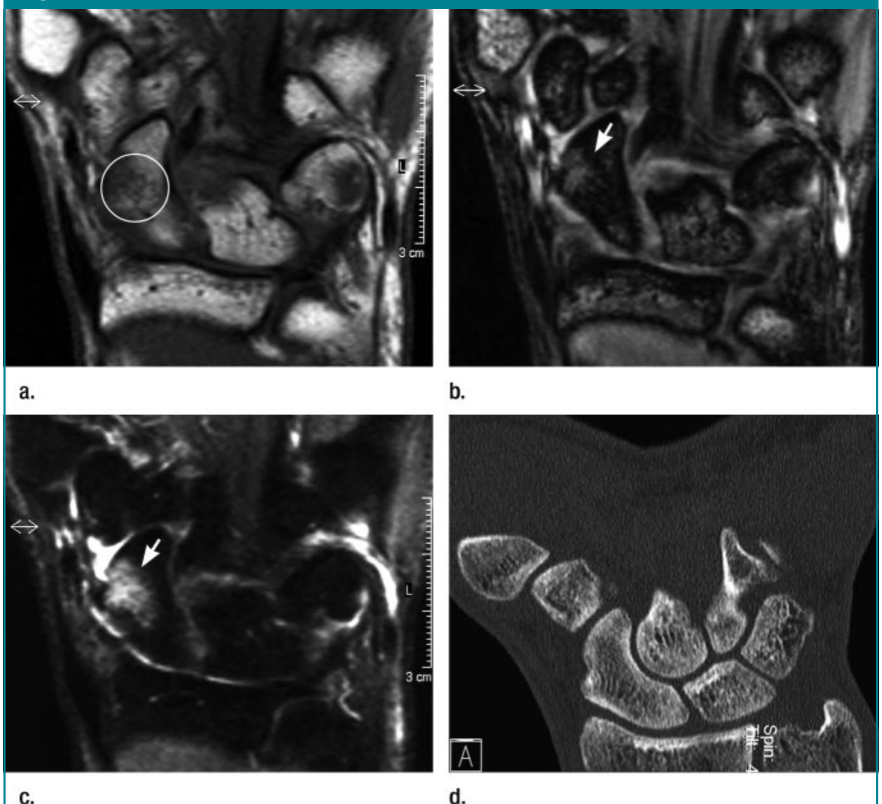

Figure 1: Trabecular scaphoid fracture in a 23-year-old man. **(a)** Coronal T1-weighted (500/20) MR image obtained 2 days after trauma shows hypointense network of lines (circle) in the middle third of scaphoid bone. Coronal **(b)** T2-weighted three-dimensional gradient-echo (60/17, 20° flip angle) and **(c)** STIR (1200/13/130) MR images show highly increased signal intensity in the bone marrow (arrow). **(d)** Multidetector CT scan shows no sign of fracture.

Reference Standard

The final clinical diagnosis was established by the two radiologists in consensus, who reviewed the follow-up radiographs obtained in four planes 6 weeks after trauma. An abnormal lucent line within a bone was considered evidence of a fracture. A fracture was considered cortical if there was a break in the continuity of the cortex, a sharp step in the cortex, or a dislocation of bone fragments. A fracture was considered purely trabecular if no such signs of cortical involvement could be found.

Traumatology department records, reports of surgical procedures, hospital discharge summaries, hospital charts, and the hospital's computerized clinical database were reviewed to compare our final diagnosis against the final diagnosis of the trauma surgeons.

Statistical Analysis

Data were analyzed with a statistical software package (SPSS, release 11.05; SPSS, Chicago, Ill). Sensitivity, specificity, and accuracy, as well as the corresponding 95% confidence interval (CI) were calculated by using Confidence Interval Analysis software (version 2.1.2; Trevor Bryant, University of Southampton, England). A binomial test was used to evaluate the significance of the differences between MR imaging and multidetector CT with regard to the detection of scaphoid fractures and cortical involvement at a *P* value of less than .05.

Figure 2

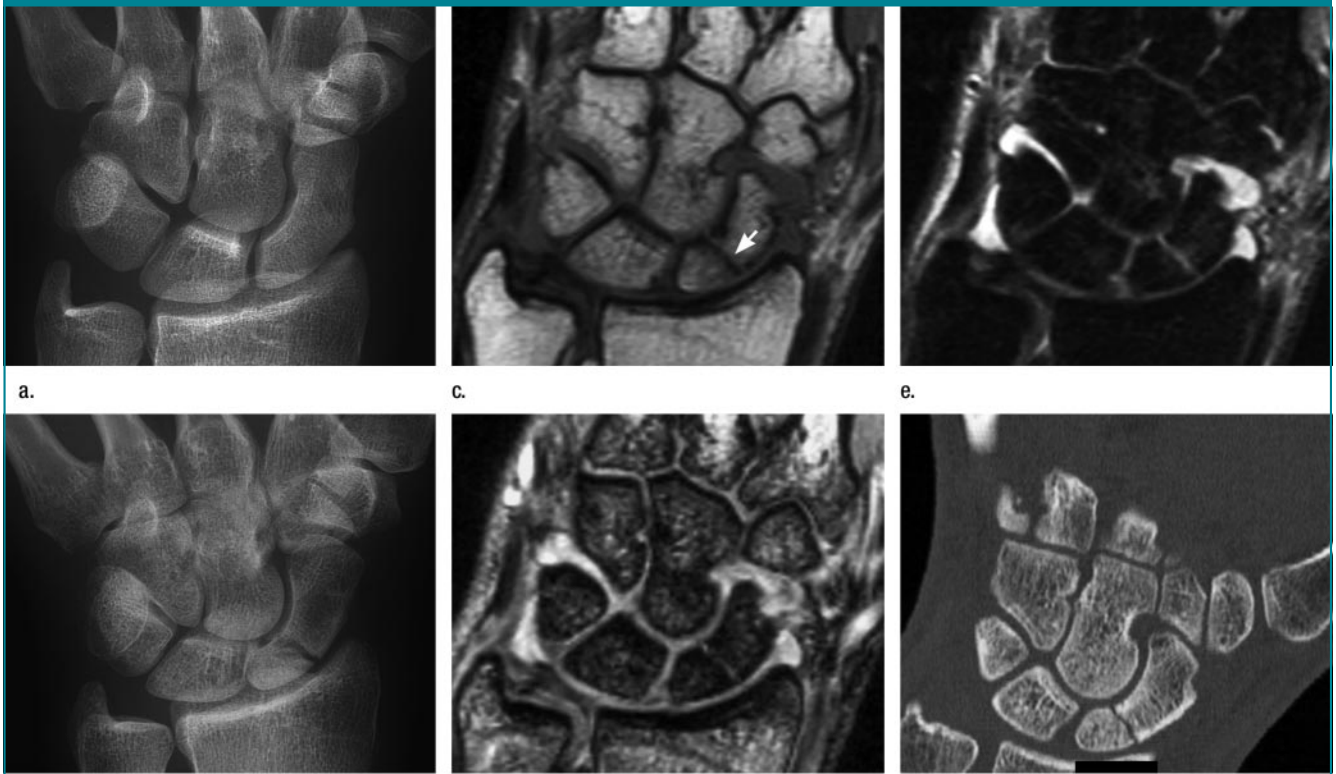

Figure 2: Complete scaphoid fracture in a 25-year-old man. **(a)** Initial conventional radiograph is negative; **(b)** after 6 weeks, a clear fracture line could be seen. Coronal **(c)** T1-weighted (500/20), **(d)** T2-weighted three-dimensional gradient-echo (60/17, 20° flip angle), and **(e)** STIR (1200/13/130) MR images obtained 4 days after trauma demonstrate complete cortical and trabecular fracture line in the scaphoid bone that is hypointense on **c** (arrow) and hyperintense on **d** and **e**. **(f)** Coronal multiplanar reformation from multidetector CT performed on the same day shows nondisplaced fracture of the scaphoid.

Results

Final Diagnosis

On 6-week follow-up radiographs, a fracture of at least one wrist bone was seen in 20 (69%) of the 29 patients; no signs of osseous injury were seen in nine (31%) patients.

A scaphoid fracture was seen in 11 (38%) of 29 patients (Table 1). The scaphoid fractures were located in the distal third of the bone in four cases, in the middle third in five cases, and in the proximal third in two cases. The fractures were horizontal in four cases and oblique in seven cases. Three of the 11 patients with scaphoid fractures had evidence of trabecular involvement only, while the other eight patients had radiographic signs of cortical involvement. None of these fractures was displaced. Two of the 11 patients with scaphoid fractures had additional injuries in other wrist bones.

A total of 13 fractures were found in other wrist bones, including the radius. All of these fractures were occult, that is, not seen on the initial radiographs. The other fractures were located in the distal radius in six (17%) patients; in the triquetral bone in two (7%) patients; in the lunate bone in two (7%) patients; and in the capitate, hamate, and pisiform bone in one patient each (Table 2). Three patients had injuries in more than one bone: one patient had a fracture of the triquetral bone and the pisiform bone, one had a fracture of the triquetral bone and the scaphoid bone, and one patient had a fracture of the distal radius and the scaphoid bone. Signs of cortical involvement on the follow-up radiographs were seen in five of 13 fractures in the other wrist bones.

Our final diagnosis after 6 weeks was identical to the final diagnosis of the trauma surgeons in all patients.

MR Imaging

MR imaging helped correctly identify and localize all 11 occult scaphoid fractures that were later verified on 6-week follow-up radiographs, which resulted in 100% sensitivity (95% CI: 82%, 100%) and 100% specificity (95% CI: 87%, 100%) for the detection of fractures (Tables 1 and 3). No false-positive diagnosis was made with MR imaging.

In three (10%) of the 29 patients, MR imaging depicted diffuse edema of the wrist bones as the only sign of injury, but no osseous abnormalities were subsequently seen on follow-up radiographs. Seven (24%) of the 29 patients had no signs of osseous injury at MR imaging. In the 11 patients with occult scaphoid fractures, MR imaging depicted a trabecular fracture line associated with perifocal bone edema as a hyperintense structure alteration on STIR images and as a hypointense or hyperintense structure alteration on three-dimensional T2-weighted gradient-echo images (Fig 1). In two patients, a cortical fracture line could be identified on T1-weighted spin-echo images (Fig 2). In six patients with proved cortical involvement on follow-up radiographs, no cortical fracture line could be seen on images obtained with any of the sequences (Fig 3), which resulted in a sensitivity of 38% (95% CI: 16.0%, 65.0%), a specificity of 100% (95% CI: 52%, 100%), and an accuracy of 55% (95% CI: 24%, 85%) for the detection of cortical involvement in occult scaphoid fractures (Table 3).

Eleven of the 13 other wrist bone fractures were correctly diagnosed with MR imaging. Two cortical fractures involving the pisiform and triquetral bone were missed. This resulted in a sensitivity of 85%, a specificity of 100%, and an accuracy of 84% for detecting other occult wrist fractures with MR imaging.

Multidetector CT

Multidetector CT depicted all eight scaphoid fractures with cortical involvement, resulting in 100% sensitivity (95% CI: 75%, 100%) and specificity (95% CI: 52%, 100%) for the identification of cortical involvement (Table 3, Fig 3). Multidetector CT was significantly (P = .03) superior to MR imaging in the detection of cortical involvement. However, multidetector CT failed to depict any of the three purely trabecular fractures (Table 1). The difference between CT and MR imaging in the detection of any type of scaphoid fracture did not reach significance (P = .25). Multidetector CT revealed no false-positive findings, thus resulting in an overall sensitivity of 73% (95% CI: 48%, 89%), an overall specificity of 100% (95% CI: 87%, 100%), and an accuracy of 89% (95% CI: 78%, 100%) for the detection of scaphoid fractures (Table 3).

Multidetector CT depicted five of the 13 other fractures in the region of the wrist, all of which were characterized by cortical involvement. They were located in the lunate bone in two patients, in the distal radius in one patient, and in the triquetral and pisiform bone in one patient each. The remaining eight fractures, which were purely trabecular, were missed with CT (Table 2).

Figure 3

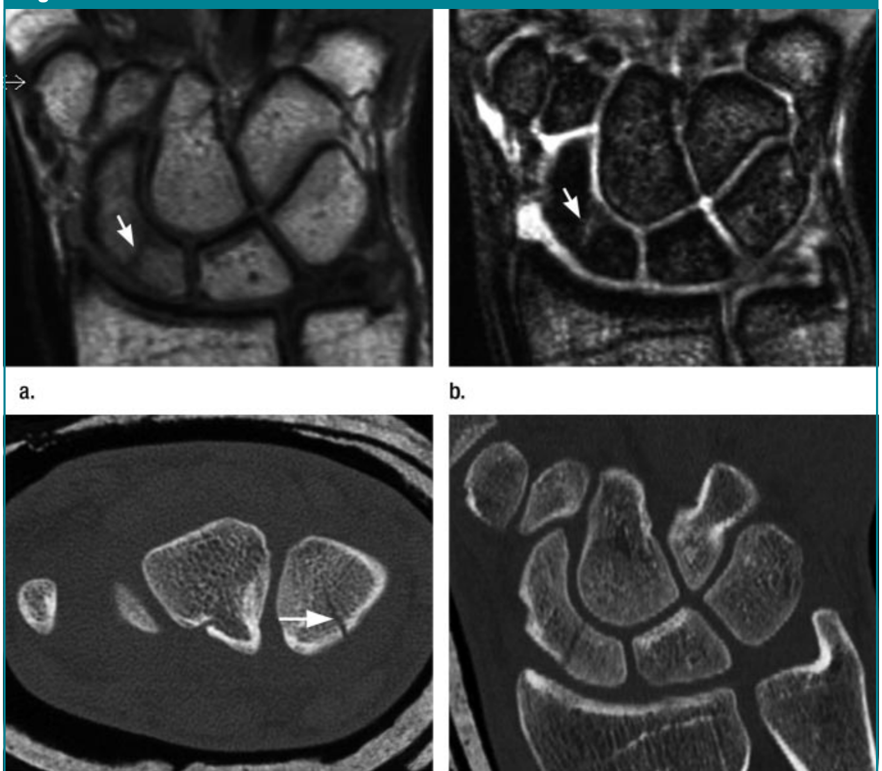

a. b. c. d.

Figure 3: Cortical scaphoid fracture in a 36-year-old woman. **(a)** Coronal T1-weighted (500/20) MR image obtained 6 days after trauma shows hypointense fracture line (arrow) in the scaphoid bone. **(b)** Coronal T2-weighted three-dimensional gradient-echo (60/17, 20° flip angle) MR image demonstrates hyperintense fracture line (arrow). Although medial extension of the fracture line could be postulated retrospectively, cortical disruption was not diagnosed prospectively. **(c)** Transverse multiplanar reformation from multidetector CT shows fracture (arrow) involving dorsal cortex of the scaphoid, which is also seen on **(d)** CT coronal multiplanar reformation.

Discussion

Multidetector CT offers excellent spatial resolution and multiplanar reformation capabilities (26,30); therefore, we studied whether this technique may be another alternative modality for imaging occult scaphoid fractures.

While our results for MR imaging are in keeping with previous reports (sensitivity and specificity of 100% relative to fracture diagnosis on 6-week follow-up radiographs), we found that the sensitivity of multidetector CT appears inferior (73%) when it comes to detection of any type of occult scaphoid fracture, be it trabecular or cortical. These results, however, are not statistically significant because of the small number of cases in which there was a discrepancy between multidetector CT and MR imaging. On the other hand, multidetector CT proved to be superior in the detection of cortical involvement of occult scaphoid fractures: Although multidetector CT could depict all eight cortical fractures, MR imaging allowed distinction between cortical and trabecular scaphoid fractures in only two cases.

A similar trend was seen for fractures of other wrist bones: Although MR imaging was more sensitive in depicting an occult fracture, multidetector CT was better able to distinguish between cortical and purely trabecular fractures. Although MR imaging missed two cortical fractures, multidetector CT was able to depict all such lesions.

According to the literature, fracture pattern is an important factor in determining the ability of a scaphoid fracture to heal (31). A stable or incomplete fracture without cortical involvement is less likely to result in nonunion (31). On the other hand, if signs of displacement are evident at initial evaluation of an acute scaphoid fracture, nonunion is more likely and requires different treatment strategies (31,32). Cortical discontinuity in a nondisplaced fracture should increase the risk of instability compared with a purely trabecular fracture. However, to our knowledge, no clinical studies are yet available that prove this point. It might even be possible that purely trabecular fractures require a shorter period of immobilization or no immobilization at all. If no immobilization is required, multidetector CT should be fully sufficient for helping make a final therapeutic decision. At present, however, patients are immobilized whenever a fracture—be it cortical or trabecular—is detected. Because MR imaging was able to depict all fractures while multidetector CT missed three purely trabecular fractures, MR imaging at present appears to be superior in helping decide whether immobilization is necessary. Since the effects of the type of nondisplaced fractures on prognosis or treatment have not yet been studied, the implications of our work cannot yet be fully determined.

A limitation of this study was the relatively small number of occult scaphoid fractures examined, which prevents us from making a definitive statement about the value of multidetector CT for exclusion of fractures when there is a clinical suspicion of a scaphoid fracture. The difference between multidetector CT and MR imaging in the detection of occult fractures was highly suggestive but did not reach a level of significance and, therefore, should be validated in future studies. The advantage of multidetector CT for detecting cortical fractures, however, is significant, even with our relatively low number of cases.

As a consequence, a positive multidetector CT scan appears sufficient for making a final diagnosis of an occult wrist fracture, but a negative multidetector CT scan does not help rule out a purely trabecular fracture and may require further evaluation. MR imaging, on the other hand, is very sensitive in depicting occult fractures and, until now, remains the standard of reference for early diagnosis of such fractures. Since most institutions use identical treatment options and immobilization periods for occult nondisplaced cortical and purely trabecular fractures, the added value of CT remains speculative. However, since CT is more readily available than MR imaging, it may assume a diagnostic role in an acute setting. CT is fast and therefore offers logistic advantages. Radiation might be a potential concern, but radiation dose for CT of the wrist is negligible if the hand is placed over the patient's head such that no other organs are in the primary beam of radiation.

In conclusion, according to our initial results, multidetector CT is a highly accurate method for detecting occult cortical scaphoid fractures and is superior to MR imaging for identifying cortical involvement, but multidetector CT appears inferior to MR imaging for identifying solely trabecular injury. Thus, a positive multidetector CT scan is diagnostic, while a negative multidetector CT scan may warrant further evaluation. Despite its excellent sensitivity, MR imaging has limitations in distinguishing trabecular from cortical fractures.

References

1. Breitenseher MJ, Gaebler C. Trauma of the wrist. Eur J Radiol 1997;25:129–139.
2. Conway WF, Destouet JM, Gilula LA, Bellinghausen HW, Weeks PM. The carpal boss: an overview of radiographic evaluation. Radiology 1985;156:29–31.
3. Dias JJ, Thompson J, Barton NJ, Gregg PJ. Suspected scaphoid fractures: the value of radiographs. J Bone Joint Surg Br 1990;72:98–101.
4. Gilula LA, Destouet JM, Weeks PM, Young LV, Wray RC. Roentgenographic diagnosis of the painful wrist. Clin Orthop Relat Res 1984;187:52–64.
5. Metz VM, Gilula LA. Imaging techniques for distal radius fractures and related injuries. Orthop Clin North Am 1993;24:217–228.
6. Yin Y, Evanoff BA, Gilula LA, Littenberg B, Pilgram TK, Kanterman RY. Surgeons' decision making in patients with chronic wrist pain: role of bilateral three-compartment wrist arthrography—prospective study. Radiology 1996;200:829–832.
7. Langhoff O, Andersen JL. Consequences of late immobilization of scaphoid fractures. J Hand Surg [Br] 1988;13:77–79.
8. Tiel van Buul MM, van Beek EJ, Broekhuizen AH, et al. Diagnosing scaphoid fractures: radiographs cannot be used as a gold standard! Injury 1992;23:77–79.
9. Breitenseher MJ, Metz VM, Gilula LA, et al. Radiographically occult scaphoid fractures: value of MR imaging in detection. Radiology 1997;203:245–250.
10. Staniforth P. Scaphoid fractures and wrist pain: time for new thinking [editorial]. Injury 1991;22:435–436.
11. Kukla C, Gaebler C, Breitenseher MJ, Trattnig S, Vecsei V. Occult fractures of the scaphoid: the diagnostic usefulness and indirect economic repercussions of radiography versus magnetic resonance scanning. J Hand Surg [Br] 1997;22:810–813.
12. Bain GI, Bennett JD, Richards RS, Slethaug GP, Roth JH. Longitudinal computed tomography of the scaphoid: a new technique. Skeletal Radiol 1995;24:271–273.
13. Fowler C, Sullivan B, Williams LA, McCarthy G, Savage R, Palmer A. A comparison of bone scintigraphy and MRI in the early diagnosis of the occult scaphoid waist fracture. Skeletal Radiol 1998;27:683–687.
14. Hodgkinson DW, Nicholson DA, Stewart G, Sheridan M, Hughes P. Scaphoid fracture: a new method of assessment. Clin Radiol 1993;48:398–401.
15. Metz VM, Wunderbaldinger P, Gilula LA. Update on imaging techniques of the wrist and hand. Clin Plast Surg 1996;23:369–384.
16. Roolker L, Tiel van Buul MM, Broekhuizen TH. Is intrasound vibration useful in the diagnosis of occult scaphoid fractures? J Hand Surg [Am] 1998;23:229–232.
17. Tiel van Buul MM, van Beek EJ, Dijkstra PF,

Bakker AJ, Broekhuizen TH, van Royen EA. Significance of a hot spot on the bone scan after carpal injury: evaluation by computed tomography. Eur J Nucl Med 1993;20:159–164.

18. Waizenegger M, Wastie ML, Barton NJ, Davis TR. Scintigraphy in the evaluation of the "clinical" scaphoid fracture. J Hand Surg [Br] 1994;19:750–753.

19. Herneth AM, Siegmeth A, Bader TR, et al. Scaphoid fractures: evaluation with high-spatial-resolution US—initial results. Radiology 2001;220:231–235.

20. Munk PL, Lee MJ, Janzen DL, et al. Gadolinium-enhanced dynamic MRI of the fractured carpal scaphoid: preliminary results. Australas Radiol 1998;42:10–15.

21. Van Gelderen W, Gale RS, Steward AH. Short tau inversion recovery magnetic resonance imaging in occult scaphoid injuries: effect on management. Australas Radiol 1998;42:20–24.

22. Hunter JC, Escobedo EM, Wilson AJ, Hanel DP, Zink-Brody GC, Mann FA. MR imaging of clinically suspected scaphoid fractures. AJR Am J Roentgenol 1997;168:1287–1293.

23. Brydie A, Raby N. Early MRI in the management of clinical scaphoid fracture. Br J Radiol 2003;76:296–300.

24. Nikken JJ, Oei EH, Ginai AZ, et al. Acute wrist trauma: value of a short dedicated extremity MR imaging examination in prediction of need for treatment. Radiology 2005;234:116–124.

25. Quinn SF, Belsole RJ, Greene TL, Rayhack JM. Advanced imaging of the wrist. RadioGraphics 1989;9:229–246.

26. Hu H, He HD, Foley WD, Fox SH. Four multidetector-row helical CT: image quality and volume coverage speed. Radiology 2000;215:55–62.

27. Tiel-van Buul MM, van Beek EJ, Borm JJ, Gubler FM, Broekhuizen AH, van Royen EA. The value of radiographs and bone scintigraphy in suspected scaphoid fracture: a statistical analysis. J Hand Surg [Br] 1993;18:403–406.

28. Hindman BW, Kulik WJ, Lee G, Avolio RE. Occult fractures of the carpals and metacarpals: demonstration by CT. AJR Am J Roentgenol 1989;153:529–532.

29. Andrews CL. From the RSNA refresher courses: evaluation of the marrow space in the adult hip. RadioGraphics 2000;20(Spec Issue):S27–S42.

30. Breederveld RS, Tuinebreijer WE. Investigation of computed tomographic scan concurrent criterion validity in doubtful scaphoid fracture of the wrist. J Trauma 2004;57:851–854.

31. Pao VS, Chang J. Scaphoid nonunion: diagnosis and treatment. Plast Reconstr Surg 2003;112:1666–1676.

32. Cooney WP 3rd. Scaphoid fractures: current treatment and techniques. Instr Course Lect 2003;52:197–208.